

## FEDSM-ICNMM2010-1000

### INTELLIGENT REGIME RECOGNITION IN UPWARD VERTICAL GAS-LIQUID TWO PHASE FLOW USING NEURAL NETWORK TECHNIQUES

**Soheil Ghanbarzadeh**

M.Sc. Student  
School of Mechanical Engineering  
Sharif University of Technology  
Tehran, Iran

**Pedram Hanafizadeh**

PhD Candidate  
School of Mechanical Engineering  
Sharif University of Technology  
Tehran, Iran

**Mohammad Hassan Saidi**

Professor and Chairman  
School of Mechanical Engineering  
Sharif University of Technology  
Tehran, Iran

**Ramin Bozorgmehry Boozarjomehry**

Associate Professor  
School of Chemical and Petroleum Engineering  
Sharif University of Technology  
Tehran, Iran

#### ABSTRACT

In order to safe design and optimize performance of some industrial systems, it's often needed to categorize two-phase flow into different regimes. In each flow regime, flow conditions have similar geometric and hydrodynamic characteristics. Traditionally, flow regime identification was carried out by flow visualization or instrumental indicators. In this research 3 kind of neural networks have been used to predict system characteristic and flow regime, and results of them were compared: radial basis function neural networks, self organized and Multilayer perceptrons (supervised) neural networks. The data bank contains experimental pressure signal for a wide range of operational conditions in which upward two phase air/water flows pass to through a vertical pipe of 5cm diameter under adiabatic condition. Two methods of signal processing were applied to these pressure signals, one is FFT (Fast Fourier Transform) analysis and the other is PDF (Probability Density Function) joint with wavelet denoising. In this work, from signals of 15 fast response pressure transducers, 2 have been selected to be used as feed of neural networks. The results show that obtained flow regimes are in good agreement with experimental data and observation.

#### INTRODUCTION

Two-phase flow is ubiquitous in many industrial processes such as petroleum, chemical engineering, metallurgy, and circumstance protection. Flow pattern monitoring plays an

important role in process control, quality assurance and safety management for two-phase flow. Vertical two-phase flow may be categorized into four major flow regimes based on their appearances: bubbly, slug, churn, and annular. The main difference between slug and churn flow can be investigated as the turbulence and vibrations in churn flow are much higher than the slug flow. Normally, hydrodynamic and kinematic mechanisms change with these flow regimes. From the point of view of theoretical analysis, in a two-fluid model, almost every constitutive relation depends on flow regime because physical mechanisms vary with flow regime transitions.

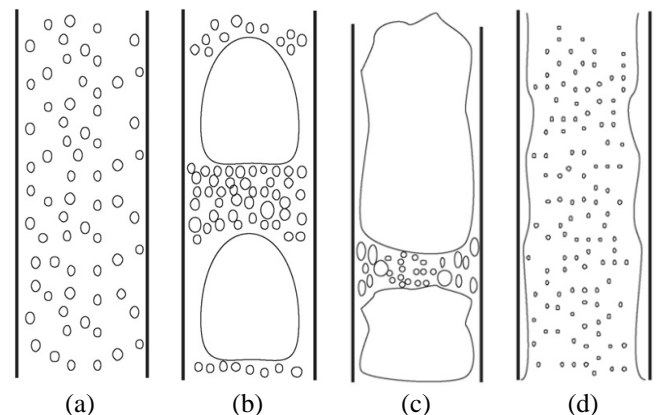


Fig.1. Two phase flow regimes in vertical pipe: a. bubbly, b. slug, c. churn and d. annular.

In this regards, many works have been done to classify flow regimes. Different ways have been used for this classification such as neutron radio graph, impedance measurement, void fraction analysis and etc. Haojiang Wu et al. [1] measured differential pressure signals of oil-gas-water multiphase flow in a horizontal pipe with a piezo-resistance differential pressure transducer. They obtained the characteristic vectors of various flow regimes are from the denoised differential pressure signals with fractal theory. In their work the characteristic vectors of known flow regimes are fed into a neural network for training. Then, the characteristic vector of some kind of unknown flow regime of oil-gas-water multiphase flow is fed into the neural network and the neural network can automatically send out the information in respect to the classification of flow regime.

Mi et al. [2] focused on developing a methodology of online flow regime identification with neural network systems trained with input from numerical simulation, which is based on theoretical models and advanced experimental techniques. In their paper the applicability of both supervised and self-organized neural networks for this method was tested. To train neural networks, they generated known input through numerical simulation of the impedance of idealized twophase flows. The carried out simulation was mainly based on two-phase theoretical models, such as the drift flux model [3-4], the newly developed slug flow model [5] and two-phase experimental databases. In another work by T. Xie et al. [6] the feasibility of a transportable artificial neural network (ANN) based technique for the classification of flow regimes in three phase gas/liquid/pulp fiber systems by using pressure signals as input was examined. Local pressure fluctuations were recorded at three different stations along the column using three independent but principally similar transducers. An ANN was designed, trained and tested for the classification of the flow regimes using as input some density characteristics of the normalized pressure signals and was shown to predict the flow regimes with good accuracy. In a recent work by Chunguo and Qiuguo [7], the gamma ray scattering energy spectrum detected by one detector was presented to distinguish the gas liquid two-phase flow regime of vertical pipe. The simulation geometries of the gamma ray scattering measurement were built using Monte Carlo software GEANT4. Their results show that the scattering energy characters of homogeneous flow and annular flow have significantly different. The scattering spectrum of slug flow is similar to annular flow for long gas slugs and similar to homogeneous flow for short gas slugs. Also in their paper the RBF neural networks were used to predict the flow regime. It was demonstrated that the method of one detector scattering energy spectrum has the ability to identify the typical gas liquid flow regime of vertical pipe and fit the applications in engineering.

In a work done by Julia et al. [8] a new approach has been used to identify both global and local flow regimes in a two-phase upward flow under adiabatic conditions. In this method, the bubble chord length distributions, which are measured simultaneously with three double-sensor conductivity probes,

have been used to feed a self-organized neural network. The global flow regime identification results show a reasonable agreement with the visual observation for all the flow conditions. Nonetheless, in this work only the local flow regimes measured at the center of the pipe agree with the global ones. Malayeri et al. [9] used radial basis function neural networks to predict cross-sectional and time-averaged void fraction at different temperatures. Their work was based on experimental measurements for a wide range of operational conditions in which upward two-phase air/water flows pass through a vertical pipe. In this article the independent parameters are in terms of dimensionless groups such as modified volumetric flow ratio, density difference ratio, and Weber number. Bai et al. [10] proposed the prerequisite to realize the online recognition. Also they obtained recognition rules for partial flow pattern based on the massive experimental data. They calculated standard templates for every flow regime feature with self-organization cluster algorithm. In this paper the multi-sensor data fusion method is presented to realize the online recognition of multiphase flow regime with the pressure and differential pressure signals, which overcomes the severe influence of fluid flow velocity and the oil fraction on the recognition.

In another work an instantaneous and objective flow regime identification method for the two-phase flow is represented by Lee et al. [11]. The previous methods have been evolved to be an objective by replacing the heuristic determination using the sensor signals in terms of the statistical indexes. The design of the neural network fed by the preprocessed impedance signals of the cross-sectional void fraction is proposed in this paper to satisfy the requirement of both objective and an instantaneous identification. It was found that the proposed flow regime identifier could successfully identify the flow regime using the short term observation data within 1 second. They also found that other flow regimes have strong dependency on the pipe diameter and some phenomena related to the kinematic wave propagation which was not considered reasonably in the previous criteria. Li [12] attempted to combine Empirical Mode Decomposition (EMD) and back propagation (BP) neural network to solve two phase flow regime identification problem. Differential pressure signal of two-phase flow, which is representatively non-stationary and multi-component signal, contains much information about flow. In mentioned work EMD is applied to differential pressure signal to obtain frequency components with different scales. The normalized energy of frequency components is extracted as features. Five flow patterns such as bubble flow, plug flow, stratified flow, slug flow and annular flow are investigated using BP neural network.

In this work we present a new method of signal processing were applied to pressure signals of two phase flow which are obtained from a large scale vertical test apparatus. Then extracted characteristic of signals were fed to three different neural networks and their performance for predicting flow regimes were observed. From results, it is obvious that these methods are acceptable and accurate.

## EXPERIMENTAL SET-UP

The experimental apparatus is shown schematically in Fig.2. The air and water were used as the gas and liquid phases in the experiments. The water is pumped from the main tank by the centrifugal pump via the strainer. To prevent vibration of the system, two shock absorbers are placed at the inlet and outlet of the pump. The water flow rates were regulated by two globe valves and were measured by the calibrated magnetic flow meter [Siemens MAG5100] with an accuracy of 0.25%. The compressed air was fed by a compressor [Atlas Copco GA210] up to 6 bar continuously. The air flow rates were set and filtered by the Wilkerson filter and regulator and were measured by the calibrated Gas Turbine flow meter [Omega FTB-934] with an accuracy of  $\pm 1\%$ . Air and water are mixed together in the plenum which is made of acrylic glass and

placed at the bottom of the riser pipe. Compressed air is injected at the plenum by the porous stainless steel plate with 108 holes of 0.5 mm diameter. The overall length and internal diameter of the riser pipe are 6 m and 50 mm, respectively. In order to have the capability of visual observation of the two phase flow patterns, the riser pipe is made of a transparent acrylic glass. The water flowed upward with air through the riser and would be separated in the separation tank at the top of the riser. The air was discharged to the atmosphere and the water was returned to the main tank or to the airlift tank. The temperature of the water was kept constant at the ambient condition. The pressure of the two phase flow is measured by the 16 pressure transmitters [INDUMART, PTF106-04G100] with accuracy of 0.3% at the different position along the riser.

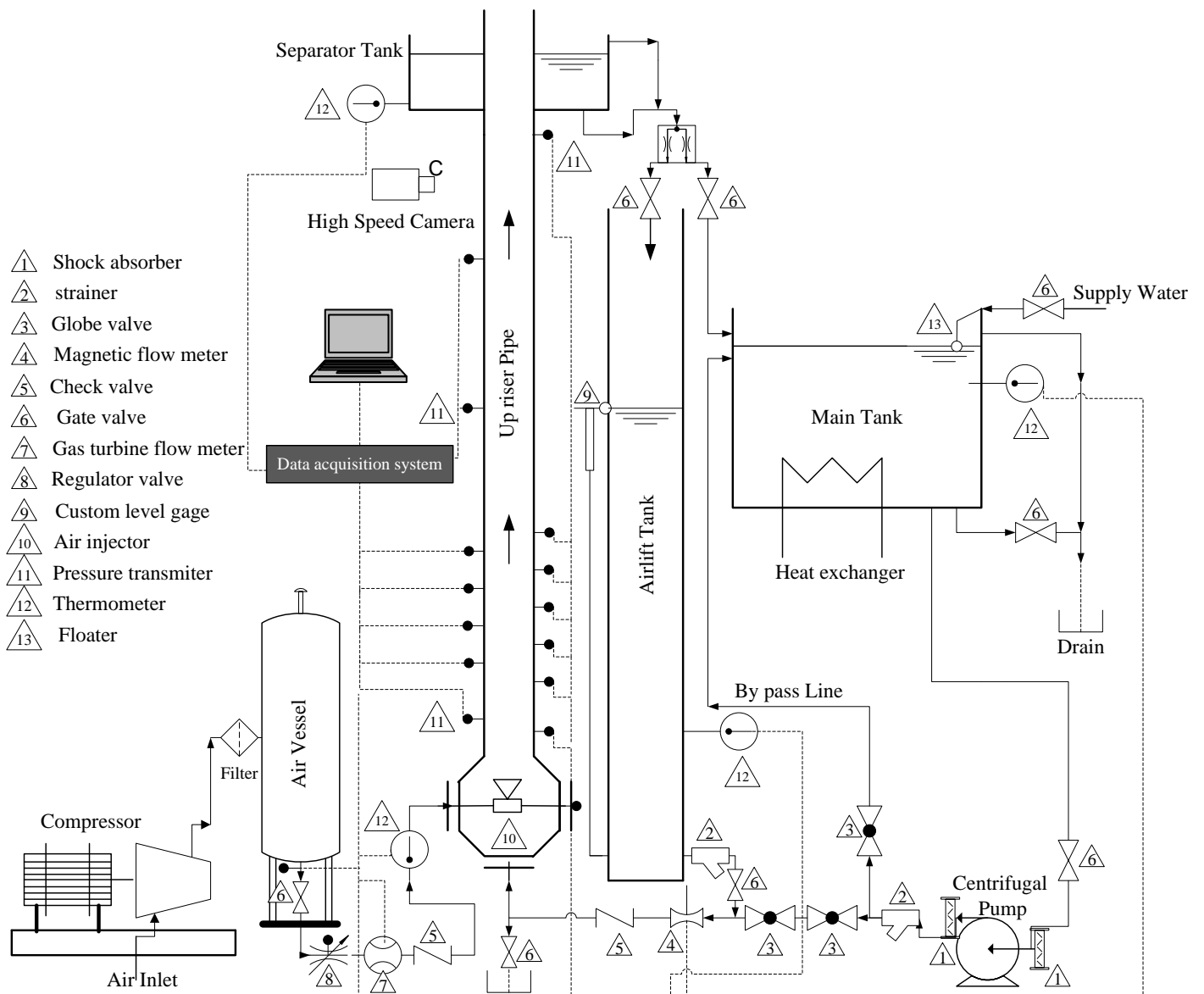


Fig.2. Schematic view for the experimental system

All the above instruments own a specified signal (4-20 mA); these signals are scaled and fed for a rapid and wide band data acquisition card of type National Instrument, PCI-6255. Recorded data are stored for further post processing. The flow regimes were observed by a high speed CCD camera [CASIO F1] with 1200 frame per second. Images were captured at the height of 5.5 m with 60 fps and resolution of 6 Mega-pixels (2816×2112). The superficial air and water velocity were set to be 0.01-10 m/s and 0.1-5 m/s, respectively.

In every test, the pressure fluctuations were recorded using the aforementioned pressure sensors, located at heights of 140cm and 175cm from the inlet of the bubble column. Acquisition frequency and length of time series data are important factors for the estimation of statistical properties of random data. The sampling frequency was selected to be 100Hz so that the Nyquist rate exceeded the maximum frequency contained in the data, as [13] suggests that the most informative pressure fluctuations in the bubble columns occur in the range from 0 to 20 Hz. The record length of 1000 data points (10s duration) was chosen on the basis of preliminary experiments to satisfy wide-sense stationarity.

### SIGNAL PROCESSING

Pressure fluctuations that result from the passage of gas and liquid pockets, and their statistical characteristics, are particularly attractive for objective characterization of flow regimes because the required sensors are robust, inexpensive and relatively well-developed, and therefore more likely to be applied in the industrial systems [13]. Power spectral density (PSD) and probability density function (PDF) of pressure drop fluctuations recorded by two pressure transducers were studied by Franca et al. [14], and more recently by Shim and Jo [15], for regime identification in gas-liquid two-phase flows. Based on the analysis of experimental data in a horizontal tube, Franca et al. [14] noted that, although PSD and PDF could not easily be used for regime identification, objective discrimination between separated and intermittent regimes might be possible by fractal techniques. Based on PSD and PDF analyses, Shim and Jo [15] could characterize bubbly, churn, and slug flow patterns in low-flow experiments in a vertical tube. At high flow rates, however, their technique could only distinguish the bubbly flow regime.

In Fig.3 pressure signals of first pressure transducer for different flow regimes are shown. As we see, these signals have different characteristics and they can be used for flow regime recognition. These are raw signals and must be denoised. Wavelet was used to denoising them.

#### Fast Fourier Transform

A Fast Fourier Transform (FFT) is an efficient algorithm to compute the Discrete Fourier Transform (DFT) and its inverse. There are many distinct FFT algorithms involving a wide range of mathematics, from simple complex-number arithmetic to group theory and number theory.

A DFT decomposes a sequence of values into components of different frequencies. This operation is useful in many fields

but computing it directly from the definition is often too slow to be practical.

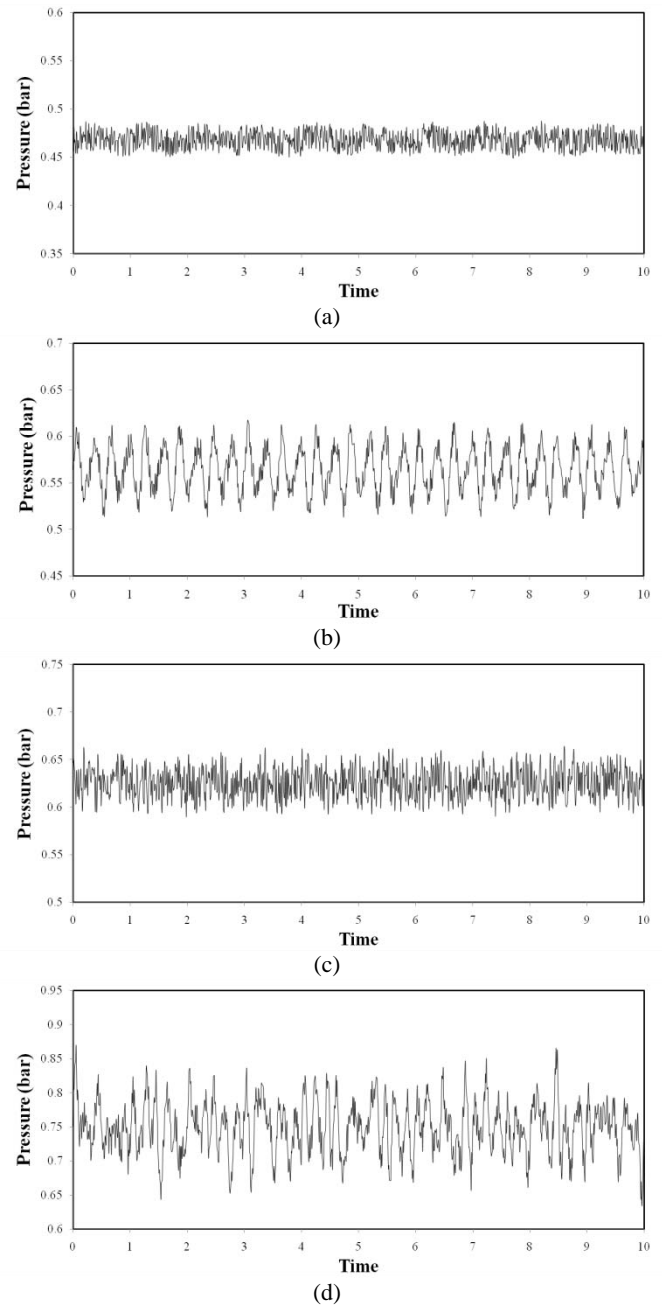


Fig.3. Pressure signal of different flow regimes, a. bubbly, b. slug, c. churn and d. annular

An FFT is a way to compute the same result more quickly: computing a DFT of  $N$  points in the obvious way, using the definition, takes  $O(N^2)$  arithmetical operations, while an FFT can compute the same result in only  $O(N \log N)$  operations. The difference in speed can be substantial, especially for long data sets where  $N$  may be in the thousands or millions—in practice,

the computation time can be reduced by several orders of magnitude in such cases, and the improvement is roughly proportional to  $N/\log(N)$ . This huge improvement made many DFT-based algorithms practical; FFTs are of great importance to a wide variety of applications, from digital signal processing and solving partial differential equations to algorithms for quick multiplication of large integers. The most well known FFT algorithms depend upon the factorization of  $N$ , but (contrary to popular misconception) there are FFTs with  $O(N \log N)$  complexity for all  $N$ . Many FFT algorithms only depend on the fact that  $e^{-\frac{2\pi i}{N}}$  is an  $N^{\text{th}}$  primitive root of unity, and thus can be applied to analogous transforms over any finite field, such as number-theoretic transforms. Since the inverse DFT is the same as the DFT, but with the opposite sign in the exponent and a  $1/N$  factor, any FFT algorithm can easily be adapted for it.

An FFT computes the DFT and produces exactly the same result as evaluating the DFT definition directly; the only difference is that an FFT is much faster. In the presence of round-off error, many FFT algorithms are also much more accurate than evaluating the DFT definition directly.

Let  $x_0, \dots, x_{N-1}$  be complex numbers. The DFT is defined by the formula

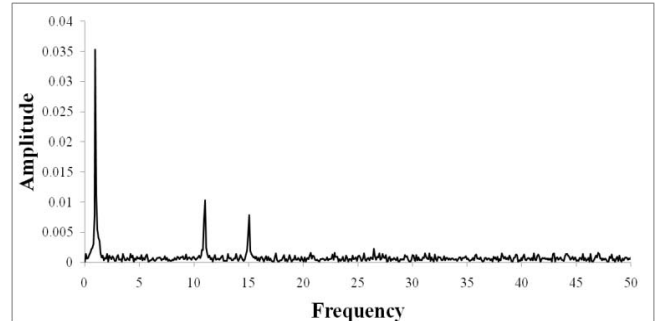
$$X_k = \sum_{n=0}^{N-1} x_n e^{-i2\pi k \frac{n}{N}}$$

Evaluating this definition directly requires  $O(N^2)$  operations: there are  $N$  outputs  $X_k$ , and each output requires a sum of  $N$  terms. An FFT is any method to compute the same results in  $O(N \log N)$  operations. More precisely, all known FFT algorithms require  $O(N \log N)$  operations (technically,  $O$  only denotes an upper bound), although there is no proof that better complexity is impossible.

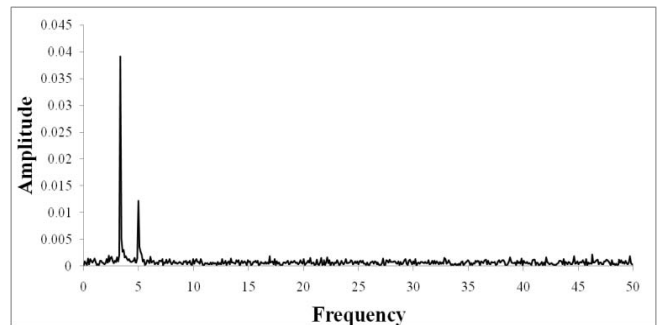
The Fourier transform produces averaged spectral coefficients that are independent of time and is useful to identify dominant frequencies in a signal. When a Fourier spectrum from the signal displays more than one peak, the information on the frequencies, at which the peaks occur, with respect to time, i.e., frequency-time plots, is very valuable to the understanding of flow physics [16-18]. This information may be given in the short fast Fourier transform. However, FFT may suffer from some limitations as mentioned in [19-22], but in this work it does an acceptable work.

Fig.4 shows a sample of the FFT of pressure signals for different flow regime. As it is seen any regimes has one or more dominant frequency in which the amplitude of FFT is maximum. The processing of more than 100 signals per each regime shows (Fig.4-a) that the dominant frequency of bubbly flow is about 1.5Hz. In spite of this fact two smaller peaks are seen in 11 and 15.2 Hz. With a good accuracy this trend repeats in other samples for bubbly flow. The amplitude of FFT coefficient in dominant frequency for different signals of bubbly flow is about 0.0315-0.367.

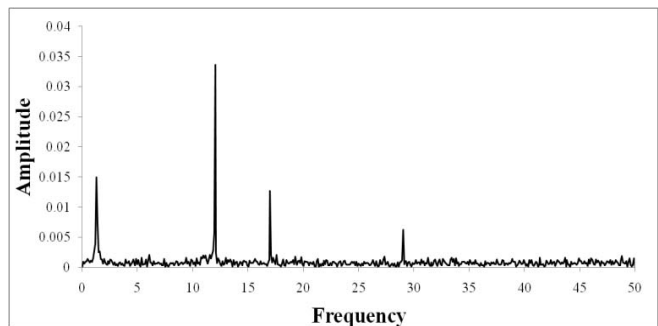
Fig.4-b represents FFT for pressure signal of slug flow. It is seen that predominant frequency occurs in 3.8Hz with amplitude of 0.039. In other signals of this regime the dominant frequency changes from 3Hz to 5.8Hz. The maximum coefficient for slug varies in range of 0.0382-0.0411.



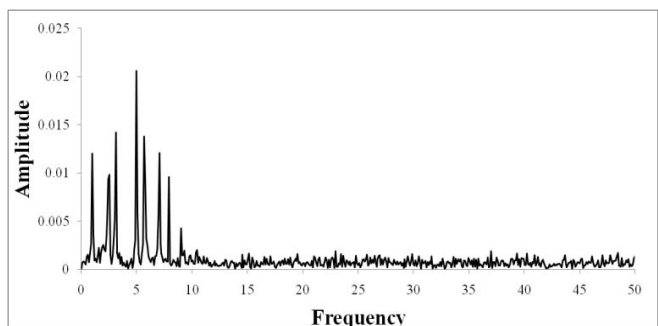
(a)



(b)



(c)



(d)

Fig.4. FFT representation of pressure signals for different flow regimes, a. bubbly, b. slug, c. churn and d. annular

For turbulent churn flow (Fig.4-c) there's 4-6 peaks in different frequency but in experiments the dominant frequency of pressure signals in this regime occurs at 11.5-12.5Hz. The nature of signals shows that the flow domain has a kind of complexity and different outstanding frequencies exist in flow. The reason can be presence of powerful turbulence in churn flow. In annular flow dominant frequencies are in range of 0-10Hz. The number of peaks varies between 6 and 10. But the amplitudes and frequencies of these peaks are close. The location of dominant frequency changes for different run of annular flow but it is always below 7Hz.

### Probability Density Function

In probability theory, a probability density function (abbreviated as PDF) of a continuous random variable is a function that describes the relative likelihood for this random variable to occur at a given point in the observation space. The probability of a random variable falling within a given set is given by the integral of its density over the set. On rare occasions the term "probability distribution function" is used to denote the probability density function. However special care should be taken around this term, since the "probability distribution function" may be used when the probability distribution is defined as function over general sets of values, or it may refer to the cumulative distribution function, or it may be a probability mass function rather than the density.

A PDF is most commonly associated with continuous univariate distributions. A random variable  $X$  has density  $f$ , where  $f$  is a non-negative Lebesgue-integrable function, if

$$P[a \leq X \leq b] = \int_a^b f(x)dx$$

Hence, if  $F$  is the cumulative distribution function of  $X$ , then

$$F(x) = \int_{-\infty}^x f(u)du$$

and

$$f(x) = \frac{d}{dx}F(x)$$

Intuitively, one can think of  $f(x)dx$  as being the probability of  $X$  falling within the infinitesimal interval  $[x, x + dx]$ . This definition may be extended to any probability distribution using the measure-theoretic definition of probability. A random variable  $X$  has probability distribution  $X \sim P$ , the density of  $X$  with respect to a reference measure  $\mu$  is the Radon–Nikodym derivative

$$f = \frac{dX * P}{d\mu}$$

That is,  $f$  is any function with the property that

$$P[X \in A] = \int_{X^{-1}A} dP = \int_A f d\mu$$

for any measurable set  $A$ . The standard normal distribution has probability density

$$f(x) = \frac{e^{-\frac{x^2}{2}}}{\sqrt{2\pi}}$$

If a random variable  $X$  is given and its distribution admits a probability density function  $f$ , then the expected value of  $X$  (if it exists) can be calculated as

$$E(X) = \int_{-\infty}^{\infty} xf(x)dx$$

Not every probability distribution has a density function: the distributions of discrete random variables do not; nor does the Cantor distribution, even though it has no discrete component, i.e., do not assign positive probability to any individual point.

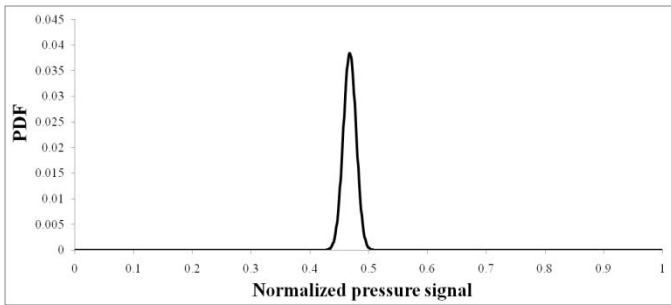
Fig.5 demonstrates PDF of normalized pressure signals for different flow regimes. As we see for bubbly flow (Fig.5-a) maximum of PDF occurs in vicinity of 0.465bar. Another important note is that band width of PDF in bubbly flow is short. This trend is repeated for other normalized signals of bubbly flow. Fig.5-b shows the PDF of pressure signal in slug flow. In comparison with bubbly, the band width is larger and location of maximum PDF occurs at vicinity of 0.57bar. Also the maximum PDF of slug is approximately 0.015 and in bubbly is 0.04. For turbulent churn flow and annular flow (Fig.5-c-d) the location of maximum PDF moves to right. For churn flow it occurs at neighboring of 0.62bar and for annular flow it occurs at 0.75bar. The band width in annular flow is larger than churn flow and its peak has a lower quantity.

The above analysis show that although raw pressure signal of flow has not capability of being used for regime detection but some simple signal processing techniques can be useful for feature extraction from this signals. The final features which were used as input of neural network are 3 dominant frequencies (if there's not 3 dominant frequencies, others were set to zero), maximum PDF, location of maximum PDF and band width of PDF.

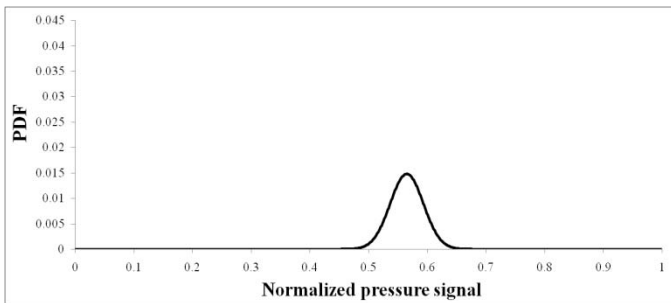
### NEURAL NETWORK ANALYSIS

To avoid subjective judgment, artificial neural network (ANN) modeling has been employed to implement non-linear mappings from measurable physical parameters to flow regimes [2, 23-24]. Artificial neural networks are analytical tools that imitate the neural aspect of the human brain, whereby learning is based on experience and repetition rather than the application of rule-based principles and formulas. An ANN

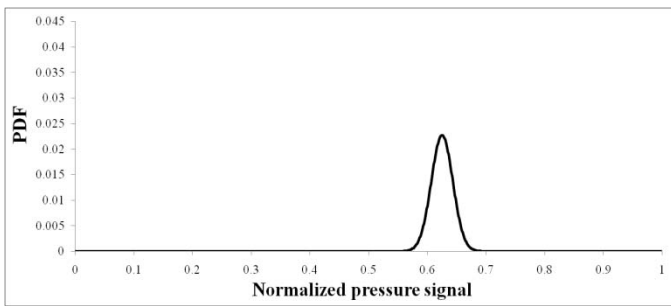
consists of a layered network of neurons (nodes), with each neuron connected to a large number of others.



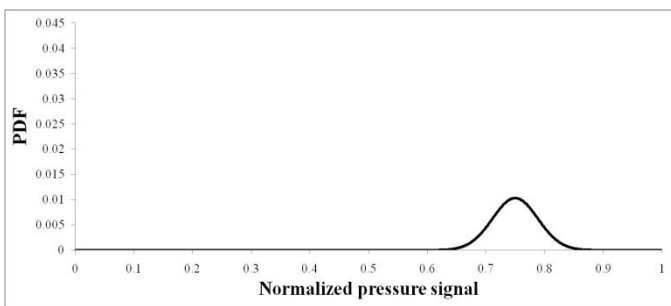
(a)



(b)



(c)



(d)

Fig.5. PDF of normalized pressure signal of different regimes, a. bubbly, b. slug, c. churn and d. annular

The input signal to the network is passed among the neurons, with each neuron calculating its own output using weighting associated with connections. Learning is achieved by the adjustment of the weights associated with inter-neuron connections. ANNs provide capabilities such as learning, self-

organization, generalization (response to new problems using incomplete information), and training; and are excellent for pattern recognition and trend prediction for processes that are non-linear, poorly-understood, and/or too complex for accurate first-principle mathematical modeling. They seem ideal for applications to multiphase flow systems, and when properly designed and trained, can potentially improve on-line monitoring and diagnostics. ANNs have recently been applied for the prediction of complex thermal systems rather extensively. Although the application of neural networks to multiphase flow problems has started only recently, the published studies have clearly demonstrated their enormous potential [6].

### Radial Basis Function Neural Network

At present, the radial basis function network is one of the main fields of research in numerical analysis [25]. This network has a fast rate of learning and high accuracy. The construction of a radial basis function network in its most basic form involves three entirely different layers. The input layer is made of input nodes. The second layer is a hidden layer of sufficient dimensions, which serves a different purpose than in multi-layer perceptrons, such as back-propagation networks. The output layer supplies the response of the network to the activation patterns applied to the input layer. A typical structural form of a RBF with multiple inputs and one output is shown in Fig.6. In contrast to the multi-layer perceptrons, the transformation from input space to the hidden layer space is non-linear, whereas the transformation from the hidden layer space to the output space is linear. RBFs are used in designing the networks and are developed in two phases, as follows

1. The training or learning phase in which a set of known input/output patterns are presented to the network. The weights are adjusted between the nodes until the desired output is provided.
2. The generalization phase in which the network is subjected to input patterns that it has not seen before, but whose outputs are known and the performance is monitored.

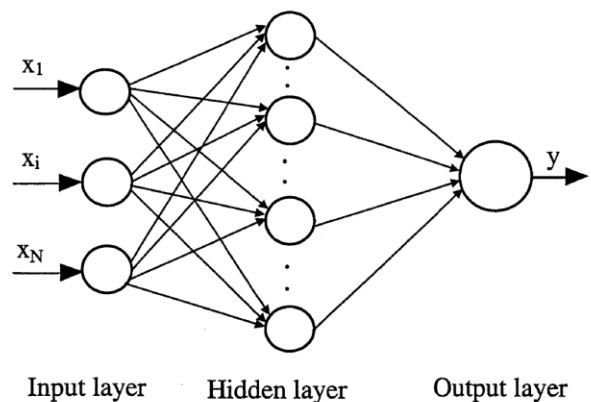


Fig.6. Schematic of RBF neural network

Input and output variables in designing the networks are to be used in terms of dimensionless groups and normalized form. Selection of input and output variables and of the data set for training should be done carefully to cover the whole range of variables, since neural networks cannot be used reliably for extrapolations. In general, the majority of data are used for training the network, and the remaining part for the generalization phase. More details about RBFs could be found in [25, 26]. Fig.7 demonstrates the training error for data sets of flow regimes.

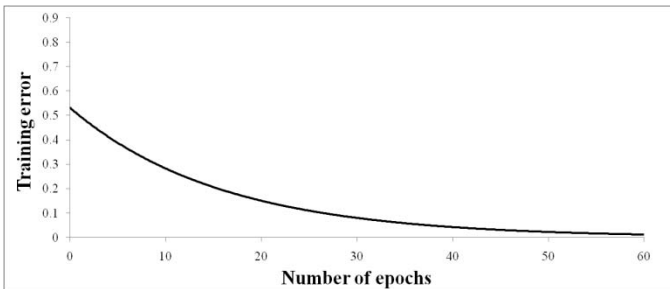


Fig.7. training error of RBF neural network for regime identification

### Self-Organized Neural Network

The self-organizing networks are often used to form clusters. No information concerning the correct class is provided to these neural networks during training. A self-organizing neural network is a two-layer network that can cluster input data into several categories that contain similar objects in the input data. The number of categories is specified subjectively. The classified results of the neural network can show the inherent relations among the patterns that feature the data involved. In this research, multiple self-organizing neural networks were employed to perform flow regime identification. In the system, there is only one neural network in the first layer, two output nodes of which are connected to the next layer. In the following layers, each neural network may have two output nodes. Once the system is set up and trained, an input may pass through a couple of layers to reach an ending node, corresponding to a specific pattern that the input should belong to. These multiple neural networks allow one to adopt more input variables since each unit may have as many as 20 input variables, and to make dominant input more effective around transition regions. Another advantage of the multiple neural networks over a single neural network is that physical understanding is embodied into each layer and each unit. In a sense of virtual classification, each unit may have its own very meaningful function [2]. Fig.8 shows a simple schematic of self-organized neural network. As shown in this figure, in the first layer, a self-organizing neural network was assigned with two output nodes to group any flow into one of two patterns. In other words, the first unit,  $U_0$ , can divide the flow regime map into two parts. After training unit  $U_0$ , the result showed that one output node corresponded to bubbly, annular and churn flows, while the other corresponded to slug flow. Unit  $U_1$  further separated the first output node of unit  $U_0$  into two nodes: one corresponded to annular and churn flows, the other

corresponded to bubbly flow. The first output nodes of unit  $U_2$  was divided into two nodes corresponding to annular and churn flow, respectively. Accordingly, after training, the neural network classified these simulated input values to output nodes corresponding to four flow regimes.

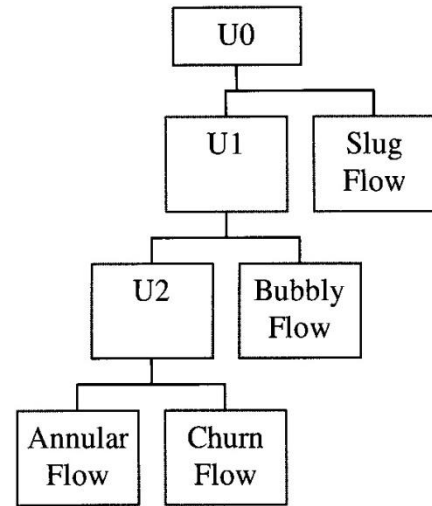


Fig.8. Schematic diagram for a four nodes self-organizing classifier of two phase flow

Fig.9 shows the clusters of regimes which were obtained due to self-organizing mapping. It shows that the flow regimes were classified properly and there's adequate distance between them.

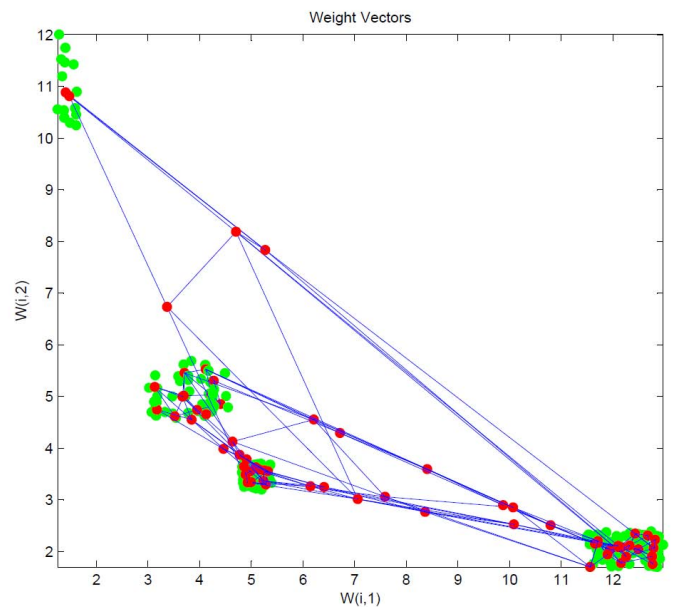


Fig.9. Two weight factors (from 6) and self organized mapping of regimes



## Multi-Layer Perceptrons (Supervised) Neural Networks

An MLP is a network of simple neurons called perceptrons. The basic concept of a single perceptron was introduced by Rosenblatt in 1958. The perceptron computes a single output from multiple real-valued inputs by forming a linear combination according to its input weights and then possibly putting the output through some nonlinear activation function. Mathematically this can be written as

$$y = \varphi \left( \sum_{i=1}^n \omega_i x_i + b \right) = \varphi(w^T x + b)$$

where  $w$  denotes the vector of weights,  $x$  is the vector of inputs,  $b$  is the bias and  $\varphi$  is the activation function.

A single perceptron is not very useful because of its limited mapping ability. No matter what activation function is used, the perceptron is only able to represent an oriented ridge-like function. The perceptrons can, however, be used as building blocks of a larger, much more practical structure. A typical multilayer perceptron (MLP) network consists of a set of source nodes forming the input layer, one or more hidden layers of computation nodes, and an output layer of nodes. The input signal propagates through the network layer-by-layer.

While single-layer networks composed of parallel perceptrons are rather limited in what kind of mappings they can represent, the power of an MLP network with only one hidden layer is surprisingly large. As Hornik et al. [27] and Funahashi[28] showed such networks, are capable of approximating any continuous function  $f: \mathcal{R}^n \rightarrow \mathcal{R}^m$  to any given accuracy, provided that sufficiently many hidden units are available.

MLP networks are typically used in supervised learning problems. This means that there is a training set of input-output pairs and the network must learn to model the dependency between them. The training here means adapting all the weights and to their optimal values for the given pairs. The criterion to be optimized is typically the squared reconstruction error

$$\sum_t \|f(s(t)) - x(t)\|^2$$

The supervised learning problem of the MLP can be solved with the back-propagation algorithm. The algorithm consists of two steps. In the backward pass, partial derivatives of the cost function with respect to the different parameters are propagated back through the network. The chain rule of differentiation gives very similar computational rules for the backward pass as the ones in the forward pass. The network weights can then be adapted using any gradient-based optimization algorithm. The whole process is iterated until the weights have converged [25].

The MLP network can also be used for unsupervised learning by using the so called auto-associative structure. This is done by setting the same values for both the inputs and the outputs of the network. The extracted sources emerge from the

values of the hidden neurons [29]. This approach is computationally rather intensive. The MLP network has to have at least three hidden layers for any reasonable representation and training such a network is a time consuming process.

Fig.10 shows the training error for regime identification versus number of epochs. As we see the training error decreases with increasing number of epochs, but this trend exists if epochs were less than 200. For more number of epochs the training error gets a periodic form.

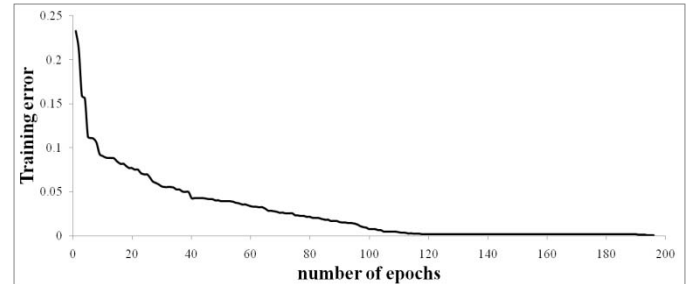


Fig.10 Training error for MLP versus number of epochs

Table 1 shows the results of checking data (more than 70 checks for each regime) for three different ANNs. The contents of table are presented in term of accuracy for prediction.

Table1. Accuracy of regime prediction for different ANNs

ANN	RBF	SOM	MLP
bubbly	100%	100%	100%
slug	97.6%	98.1%	96.9%
churn	98.1%	98.9%	97.7%
annular	97.1%	98.3%	96.2%

Table 1 show that accuracy of flow regime identification of SOM (self organizing mapping) is better than two others ANNs. But considering a note is so important here, the main error which exists in regime prediction refers to pressure signal and its post processing not to ANNs. As our data for each regime are simply distinguishable AANs do their work correctly or almost correctly. Due to different operating conditions, some features of normalized pressure signal may cause confusion.

## CONCLUSION

In this paper, flow pattern identification using RBF, SOM and MLP is discussed in detail. Some features of the differential pressure signal in different frequency scales is extracted as the characteristic of flow pattern and the mentioned neural networks completed excellently the classification task of flow pattern. Air-water two-phase flow experiment shows that neural network can characterize the complex relationship between flow pattern and the differential pressure signal with satisfactory accuracy.

## ACKNOWLEDGMENT

The authors would like to express their sincere appreciation to Mrs. P.M. Gholampour for her encouragement, support and technical comments on the subject. This research was partially supported by Iran Supplying Petrochemical Industries Parts, Equipment and Chemical Design Corporation (SPEC) grant KPR-8628077, which is gratefully acknowledged.

## REFERENCES

- [1] Wu, H., Zhou, F., Wu, Y., 2001, "Intelligent Identification System of Flow Regime of Oil-Gas-Water Multiphase Flow," *Int. J. Multiphase Flow*, Vol. 27, pp. 459-475.
- [2] Mi, Y., Ishii, M., Tsoukalas, L.H., 2001 "Flow regime identification methodology with neural networks and two-phase flow models", *J Nuclear Engineering and Design*, Vol. 204, pp. 87-100.
- [3] Zuber, N., Findlay, J.A., 1965, "Average Volumetric Concentration in Two-Phase Flow Systems," *J. Heat Transfer*, Vol. 87, pp. 453-468.
- [4] Ishii, M., 1977, "One-dimensional drift-flux model and constitutive equations for relative motion between phases in various two-phase flow regimes," ANL77-47.
- [5] Mi, Y., 1998, "Two-Phase Flow Characterization Based on Advanced Instrumentation, Neural Networks, and Mathematical Modeling," Ph.D. Thesis, Purdue University.
- [6] Xie, T., Ghiaasiaan, S.M., Karrila, S., 2004, "Artificial Neural Network Approach for Flow Regime Classification in Gas-Liquid-Fiber Flows Based on Frequency Domain Analysis of Pressure Signals," *J. Chemical Engineering Science*, Vol. 59, pp. 2241-2251.
- [7] Chunguo, J. and Qiuguo, B., 2009, "Flow Regime Identification of Gas/Liquid Two-phase Flow in Vertical Pipe Using RBF Neural Networks," proceeding of 2 Chinese Control and Decision Conference (CCDC 2009), pp. 5143-5147.
- [8] Julia, J.E., Liu, Y., Paranjape, S., Ishii, M., 2008, "Upward Vertical Two-Phase Flow Local Flow Regime Identification Using Neural Network Techniques," *J. Nuclear Engineering and Design*, Vol. 238, pp. 156-169.
- [9] Malayeri, M.R., Muller-Steinhagen, H., Smith, J.M., 2003, "Neural Network Analysis of Void Fraction in Air/Water Two Phase Flows at Elevated Temperatures," *Chemical Engineering and Processing*, Vol. 42, pp. 587-597.
- [10] Bai, B., Zhang, S., Zhao, L., Zhang, X., Guo, Li., 2008, "Online Recognition of the Multiphase Flow Regime," *J. Science in China Series E: Technological Sciences*, Vol. 51, No. 8, pp. 1186-1194.
- [11] Lee, J.Y., Ishii, M., Kim, N.M., 2008, "Instantaneous and Objective Flow Regime Identification Method for the Vertical Upward and Downward Co-Current Two-Phase Flow," *International Journal of Heat and Mass Transfer*, Vol. 51, pp. 3442-3459.
- [12] Li, Q., 2008, "Flow Pattern Identification of Two-Phase Flow Using Neural Network and Empirical Mode Decomposition," *Proceeding of Fourth International Conference on Natural Computation*, pp. 375-378.
- [13] Drahos, J., Zahradnik, J., Puncocar, M., Fialova, M., Bradka, F., 1991, "Effect of Operating Conditions on the Characteristics of Pressure Fluctuations in a Bubble Column," *Chemical Engineering and Processing*, Vol. 29, pp. 107-115.
- [14] Franca, F., Acikgoz, M., Lahey Jr., R.T., Clausse, A., 1991, "The Use of Fractal Techniques for Flow Regime Identification," *Int. J. Multiphase Flow*, Vol. 17, pp. 545-552.
- [15] Shim, W., Jo, C.H., 2000, "Analysis of Pressure Fluctuations in Two-Phase Vertical Flow in Annulus," *J. Industrial and Engineering Chemistry (Seoul)*, Vol. 6, pp. 167-173.
- [16] Farge, M., 1992, "Wavelet Transforms and Their Applications To Turbulence," *Annual Review of Fluid Mechanics*, Vol. 24, pp. 395-457.
- [17] Alam, M.M., Moriya, M., Sakamoto, H., 2003, "Aerodynamic Characteristics of Two Side-by-Side Circular Cylinders And Application of Wavelet Analysis on the Switching Phenomenon," *Journal of Fluids and Structures*, Vol. 18, pp. 325-346.
- [18] Alam, M.M., Sakamoto, H., 2005, "Investigation of Strouhal frequencies of two staggered bluff bodies and detection of multistable flow by wavelets," *Journal of Fluids and Structures*, Vol. 20, pp. 425-449.
- [19] Daubechies, I., 1990, "The Wavelet Transforms, Time-Frequency Localization and Signal Analysis," *IEEE Transaction, Information Theory*, Vol. 36, pp. 961-1005.
- [20] Newland, D.E., 1993, "An Introduction of Random Vibrations, Spectral and Wavelet Analysis," third ed. London, Longman Scientific and Technical.
- [21] Hamdan, M.N., Jubran, B.A., Shabaneh, N.H., Abu-Samak, M., 1996, "Comparison of various basic wavelets for the analysis of flow induced vibration of a cylinder in cross-flow," *Journal of Fluids and Structures*, Vol. 10, pp. 633-651.
- [22] Torrence, C., Compo, G., 1998, A practical guide to wavelet analysis," *Bulletin of the American Meteorological Society*, Vol. 79, pp. 61-78.
- [23] Cai, S., Toral, H., Qiu, J., Archer, J.S., 1994, "Neural network based objective flow regime identification in air-water two-phase flow," *Canadian Journal of Chemical Engineering*, Vol. 72, pp. 440-445.
- [24] Mi, Y., Ishii, M., Tsoukalas, L.H., 1998, "Vertical two-phase flow identification using advanced instrumentation and neural networks," *Nuclear Engineering and Design*, Vol. 184, pp. 409-420.
- [25] Haykin, S.S., 1999, "Neural Networks: A Comprehensive Foundation," 2<sup>nd</sup> edition, Prentice Hall, London, UK.
- [26] Sarrafi, A., 1999, "Studies of holdup, mixing, and heat transfer in bubble column reactors," PhD thesis, University of Surrey, Guildford, UK.
- [27] Hornik, K., Stinchcombe, M., and White. H., 1989, "Multilayer feedforward networks are universal approximators," *Int. J. of Neural Networks*, Vol. 2, No. 5, pp. 359-366.
- [28] Funahashi, K., 1989, "On the approximate realization of continuous mappings by neural networks," *Int. J. of Neural Networks*, Vol. 2, No. 3, pp. 183-192.
- [29] Hochreiter, S. and Schmidhuber, J., 1999, "Feature extraction through LOCO-CODE," *Int. J. of Neural Computation*, Vol. 11, No.3, pp. 679-714.